

# An experimental parametric study on natural circulation BWRs stability



Christian P. Marcel<sup>a,b,c,\*</sup>, M. Rohde<sup>d</sup>, T.H.J.J. Van Der Hagen<sup>d</sup>

<sup>a</sup> Instituto Balseiro, 8400 S. C de Bariloche, Argentina

<sup>b</sup> Centro Atómico Bariloche, CNEA, Bustillo 9500, 8400 S. C. de Bariloche, Río Negro, Argentina

<sup>c</sup> Consejo Nacional de Investigaciones Científicas y Técnicas (CONICET), Argentina

<sup>d</sup> Department of Physics of Nuclear Reactors, Delft University of Technology (TUDelft), Delft 2629 JB, The Netherlands

## HIGHLIGHTS

- An experimental loop with artificial neutronic feedback is developed for NC-BWRs studies.
- The use of MOX fuels in BWRs may degrade their stability performance.
- Small values of the void reactivity feedback coefficient can strongly destabilize the TH-mode.
- Having a strongly destabilized TH-mode can destabilize the system when considering neutronic feedback.

## ARTICLE INFO

### Article history:

Received 10 January 2017

Received in revised form 10 April 2017

Accepted 11 April 2017

### Keywords:

Natural circulation BWR stability  
Parametric study  
Artificial void-reactivity-feedback

## ABSTRACT

A parametric study on the stability performance of a prototypical natural circulation BWR is performed with the downscaled GENESIS facility. The GENESIS design is based on fluid-to-fluid modeling and includes an artificial void reactivity feedback (VRF) system for simulating the neutronic-thermal-hydraulic coupling. In this work a more sophisticated VRF system than its predecessors is developed and implemented. The VRF allowed investigating different configurations relevant for the reactor design. The experiments show that changing the fuel rods diameter to a half (doubling) decreases (increases) the stability performance of the system while the resonance frequency increases (decreases). In addition, it is found that the use of MOX fuels in a BWR slightly decreases the stability performance of the reactor. On top of this, it is clearly observed that at least two oscillatory modes exists in the system, the thermal-hydraulic mode (associated to density waves traveling thorough the core plus chimney section) and the so-called reactor mode (related to density waves travelling thorough the core). It is observed that the last one is amplified by increasing (in an absolute sense) the void reactivity feedback coefficient. Details regarding the interplay between these oscillatory modes is also given.

© 2017 Published by Elsevier B.V.

## 1. Introduction

Next generation of nuclear reactors enhance safety by replacing active safety systems by passive ones. The Economic Simplified Boiling Water Reactor (ESBWR), being a next generation nuclear reactor, eliminates the need for circulation pumps and associated piping and systems since cooling takes place by natural circulation (Cheung et al., 1998). This cooling method is simple, inherently safe, and results in reduced overall maintenance costs. The natural circulation mechanism, however, is interwoven with other physical mechanisms such as the void/temperature-reactivity feedback,

density-waves traveling through the coolant mixture and fuel rod dynamics, each of them having their own dynamics which need to be investigated in depth (Ruspini et al., 2014).

During the design and optimization phases of novel reactor concepts, such as the ESBWR, many parameters and configurations are varied and investigated. Numerical simulations and large scale experiments are commonly used for that purpose (Paladino et al., 2002; Ishii et al., 1996). Those experiments, however, are extremely expensive and usually do not include the reactivity feedback mechanism. As a result, a lack of experimental evidence confirming numerical findings exists.

Another less expensive possibility is to use an experimental facility with a simulated neutronic feedback system. Besides the advantage regarding the operational costs of such a tool, a test facility can offer a large degree of flexibility allowing studying different configurations.

\* Corresponding author at: Centro Atómico Bariloche, CNEA, Bustillo 9500, 8400 S. C. de Bariloche, Río Negro, Argentina.

E-mail address: [christian.marcel@cab.cnea.gov.ar](mailto:christian.marcel@cab.cnea.gov.ar) (C.P. Marcel).

## Nomenclature

### Normal alphabet

$A_{1,2,3}$	gain of the corresponding transfer function
$A$	cross sectional area ( $m^2$ )
$D$	diameter (m)
$dP$	pressure drop ( $kg\ m^{-1}\ s^{-2}$ )
$f_{res}$	resonance frequency (Hz)
$G_{Conv}$	void fraction determination transfer function
$G_F$	transfer function from power to heat flux to coolant
$G_R$	Reactor transfer function from reactivity to power
$G_{TH}$	Thermal-hydraulic transfer function from power to void production
$G_{tt}$	traveling time associated transfer function
$G_{vp}$	vapor production transfer function
$l$	variable length (m)
$M$	mass flow rate ( $kg\ s^{-1}$ )
$q$	power (kW)
$q''$	heat flux ( $kW\ m^{-2}$ )
$r$	reactivity coefficient (-)
$s$	Laplace variable
$t$	time (s)
$z$	relative to the discrete form of the Laplace variable $s$

### Greek

$\alpha$	void fraction (-)
$\beta$	delayed neutron fraction (-)
$\chi$	quality (-)
$\delta$	small perturbation
$\phi$	phase ( $^\circ$ )
$\lambda$	delayed neutron decay constant ( $s^{-1}$ )
$\Lambda$	neutron generation time (s)
$\rho_{lq}$	liquid density ( $kg\ m^{-3}$ )
$\rho$	reactivity (-)
$\sigma$	real part of a pole ( $s^{-1}$ )
$\tau$	time constant (s)
$\omega$	imaginary part of a pole ( $rad\ s^{-1}$ )

### Subscripts and superscripts

$\alpha$	void fraction (-)
C	core
DC	downcomer
est	estimated
F	fuel

G	relative to GENESIS
in	inlet
$l$	liquid
meas	measured
o	outlet
rod	regarding fuel pin rod
R	reactor
tt	transit time
TH	thermal-hydraulics
vp	vapor production

### Abbreviations

BOC	Beginning of the cycle
BWR	Boiling Water Reactor
CCF	cross correlation function
DC	digital controller
DR	Decay-ratio
EPR	European Pressurized Reactor
ESBWR	Economical Simplified Boiling Water Reactor
FW	feed water
GE	General Electric Co.
GENESIS	GE natural-circulation experimental scaled facility for investigations on stability
MOC	middle of cycle
MOX	mixture oxide fuel
PC	computer
PSD	power spectral decomposition
Pu	relative to the Plutonium
U	relative to the Uranium
SB	stability boundary
SIRIUS	simulated reactivity feedback implemented into thermal-hydraulic stability facility
T-H	thermal-hydraulic
UOX	uranium oxide fuel
VRF	void reactivity feedback
ZOH	Zero – order hold

### Dimensionless numbers

$N_{PCH}$	Phase change number $N_{PCH} \equiv \frac{L q''}{A_c m_{m,o} h_{fg,o}} \frac{\rho_{l,o} - \rho_{v,o}}{\rho_{v,o}}$
$N_{sub}$	Subcooling number $N_{sub} \equiv \frac{h_{l,o,sat} - h_{l,o}}{h_{fg,o}} \frac{\rho_{l,o} - \rho_{v,o}}{\rho_{v,o}}$

During the past decade, a number of investigators performed experimental research on natural circulation BWR stability (Kok and Van der Hagen, 1999; Zboray, 2002; Furuya et al., 2004; Furuya, 2006). Furuya et al. (2004), Furuya, 2006 performed experiments in the water-based SIRIUS-N facility, containing a single heating-rod core section, a chimney section and a digital controller for mimicking the void-reactivity feedback. Zboray (2002) and Kok and Van der Hagen (1999) used the Freon-12 based DESIRE facility, representing a downscaled version of the Dodewaard-reactor (The Netherlands). This facility was equipped with a bundle geometry and a system to mimic the void reactivity feedback. SS

In recent years, a great effort has been made to construct an experimental facility that represents the ESBWR as accurately as possible. The ESBWR has therefore been downscaled to a Freon-134a based facility (GENESIS) in order to reduce the pressure, temperature and applied power to more convenient values for stability studies. A complete description of the used downscaling technique and the system for implementing the void-reactivity feedback can be found in previous works (Marcel et al., 2007; Rohde et al., 2010, 2007) and will therefore be only briefly discussed here.

Operating experimental facilities for long time allow using noise analysis techniques in order to get accurate results (Furuya

et al., 2004; Rohde et al., 2010). This approach is therefore applied here in order to study the change in stability performance when varying some design parameters.

With the GENESIS facility relevant investigations and parametric studies can be assessed, some of which will be shown in this work.

## 2. The GENESIS facility

### 2.1. The thermal-hydraulic similarity

The natural circulation BWRs stability is determined by the interplay of the flows existing in the different sections of the system with other physical mechanisms such as the void reactivity feedback, density-waves traveling through the core, the coolant mixture and the fuel rod dynamics, each of them having its own dynamics. The stability performance is therefore determined by the system as a whole. For this reason, a global similarity had to be achieved between the real reactor (ESBWR) and the experimental facility. Marcel et al. developed fluid-to-fluid downscaling rules for stability analysis focusing on such a global similarity (Marcel et al., 2007).

The GENESIS facility consists of a core section, a chimney (to enhance the natural circulation) and a downcomer section. A buffer vessel on top of the chimney provides the liquid-vapor separation. A schematic view of the GENESIS facility is shown in Fig. 1. Further technical details can be found in Table 1.

As in any boiling water reactor, in the ESBWR the presence of two-phase flow in the core has important implications for the neutronic-thermal-hydraulic coupling. However, since the GENESIS facility is equipped with electrically heated rods, to study the ESBWR reactor-kinetic stability, the neutronic feedback regarding the void-reactivity needs to be simulated.

2.2. The reactor-kinetic similarity

The GENESIS facility is extended with a system that simulates the power generation feedback due to changes in the neutronic moderation caused by vapor fluctuations in the core. This is done

**Table 1**  
Technical details of the GENESIS facility.

Parameter	Symbol, (unit)	Facility
Power per rod	$P_{rod}$ , (kW)	1.05
Pressure	$P$ , (bars)	11.4
Temperature	$T_{sat}$ (K)	317
Fuel pins per fuel bundle	NP, (-)	25
Heating rods diameter	$D_{rod}$ , (m)	0.006
Chimney hydraulic diam.	$D_{ch}$ , (m)	0.04
Fuel bundle area	$A_{fb}$ (m <sup>2</sup> )	0.002
Core mass flux (no bypass)	$G_{m,0}$ , (kg/m <sup>2</sup> s)	1001
Core hydraulic diameter	$D_h$ , (m)	0.00351
Heated length	$L_c \equiv L_{heated}$ , (m)	1.41
Chimney Length + SS	$L_R$ (m)	4.05 + 1.97
Downcomer length	$L_{DC}$ (m)	7.71
Core exit quality	$\chi_{out}$	0.169

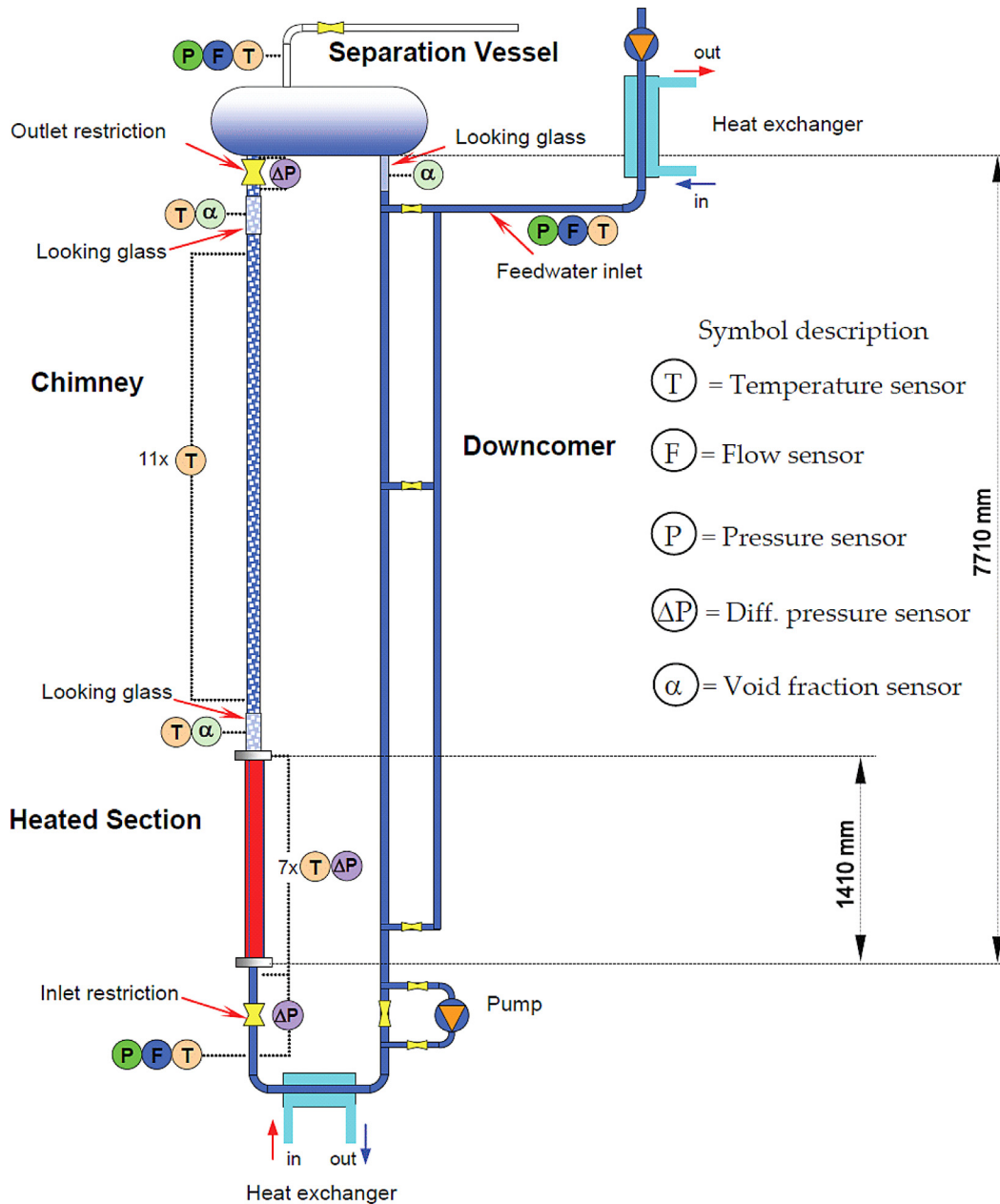
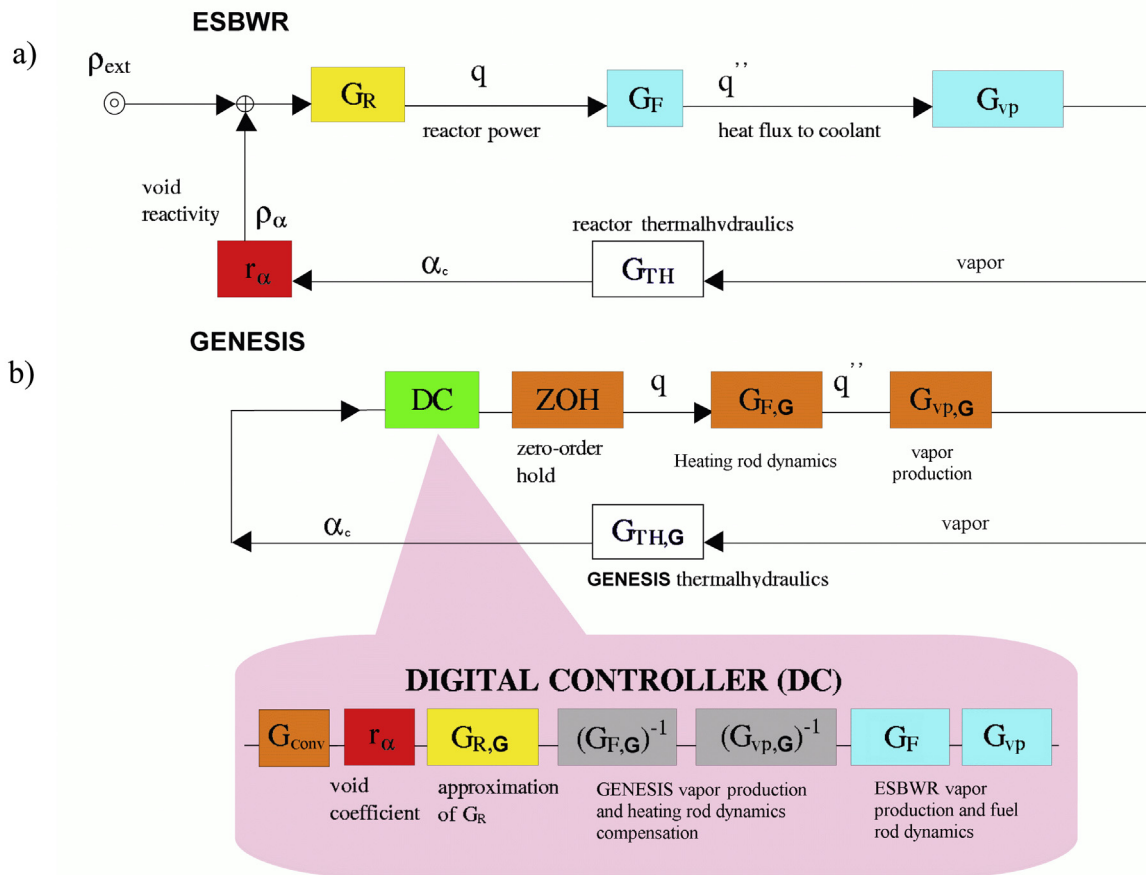


Fig. 1. Schematic view of the GENESIS facility (not to scale).

via the so-called void reactivity feedback system (VRF). Kok *et al.*, Zboray, Furuya *et al.* and Rohde *et al.* also derived VRF systems in the past (Kok and Van der Hagen, 1999; Zboray, 2002; Furuya *et al.*, 1635; Rohde *et al.*, 2010). In the GENESIS facility the VRF system adjusts the power by first estimating the core void fraction from the measured core pressure drop. Such a pressure drop is obtained from fast pressure drop sensors. This choice is based on the small phase lag introduced by these sensors with respect to the actual core-averaged void fraction (Marcel *et al.*, 2007). The VRF simulation is implemented in the form of a digital controller (DC) running on a PC. The DC controls the power of the electrically heated rods, based on the simulated reactivity effect of the measured void-fraction fluctuations.

The block diagram from Fig. 2 shows the interaction between the physical mechanisms taking place in the ESBWR and in the GENESIS facility, where  $\rho_{ext}$  stands for the external reactivity and  $\alpha_c$  for the space-averaged core void fraction. Details of the meaning of each block are given below:

- The thermal-hydraulics is represented by the  $G_{TH}$  block. Since the fluid-to-fluid modeling is such that the reactor thermal-hydraulics is correctly reproduced in the GENESIS facility, i.e.  $G_{TH,G} = G_{TH}$ .
- The space-averaged void fraction in the GENESIS core is estimated by using pressure drop sensors (process represented by  $G_{Conv}$ ) and afterwards used to calculate the void reactivity feedback due to the variation in the neutronic moderation. This feedback effect is calculated via the void reactivity coefficient (represented with  $r_\alpha$ ).
- In the GENESIS facility the neutronics is simulated by a numerical model which is solved in real time (represented by  $G_{R,G}$ ). As a result, the applied power is adjusted according to the estimated fission rate.
- Since the reactor fuel rods dynamics and the steam creation mechanism (represented by  $G_F$  and  $G_{vp}$ , respectively) influence the dynamics of the system, they are also artificially simulated in the algorithm of the VRF system. The pellet, the gap and the



- $G_R$  = Reactor transfer function from reactivity to power
- $G_F$  = Transfer function from power to heat flux to the coolant
- $G_{vp}$  = Transfer function from heat flux to coolant to void production
- $G_{TH}$  = Thermal-hydraulic transfer function from power to void production
- $r_\alpha$  = Transfer function from void fraction to reactivity
- $G_{Conv}$  = Void fraction determination transfer function
- ZOH = Zero-Order Hold
- $\alpha_c$  = Void fraction in the core
- Subscripts = GENESIS facility

Fig. 2. (a) The feedback mechanism of the ESBWR and (b) the feedback system as implemented in the GENESIS facility (adapted from Zboray (2002)).

cladding were modeled as a typical ESBWR fuel rod at MOC conditions, see (Rohde et al., 2007; Marcel et al., 2007). In addition, a boundary condition of no heat resistance at the outside of the cladding is assumed.

- Some mechanisms present in the GENESIS facility (which are absent in the reactor) need to be removed or compensated for (e.g. the heat transfer through the GENESIS heating rods and the Freon vaporization, represented by  $G_{F,G}$  and  $G_{vp,G}$ , respectively). These compensations are implemented by adding the inverse transfer functions of the mechanisms that need to be eliminated.

All the transfer functions added artificially are implemented in a discrete time form due to the discrete time characteristics of the DC. For this reason, the Z transform is used instead of the more common Laplace transform.

### 2.3. GENESIS controllability improvements

In previous works (Rohde et al., 2010, 2007, 2006; Marcel et al., 2008) many experiments have been presented for different operational points of the reference natural circulation BWR in the dimensionless plane. Due to the fact little differences may be expected in the stability performance when slightly varying a parameter, it was decided to use noise analysis techniques to investigate the stability performance of a certain configuration. From the experiments presented in Marcel et al., 2007, it was found to be difficult to operate GENESIS at a certain state for long time because of fluctuations of some input parameters (e.g. system pressure, inlet temperature, etc.) which in turn difficult the use of noise analysis and statistical tools. For that reason some modifications are introduced in the facility which improved its controllability. One of the main improvements was achieved by installing a better pressure controller system. On top of this, a by-pass system is added to the feedwater pump loop to better control cavitation of this pump together with the addition of two extra heat exchangers located at the core inlet. As a result of these modifications, the system pressure could be controlled within  $\pm 0.02$  bar and the inlet temperature within  $\pm 0.1$  °C of their respective set points.

### 2.4. Improvements in the core dynamics modeling

In previous works (Rohde et al., 2010, 2007; Marcel et al., 2007, 2008), the heat transfer through the GENESIS heating rods and the Freon vaporization (represented by  $G_{F,G}$  and  $G_{vp,G}$ , respectively) was modeled by a first-order process; thus,

$$G_{vp,G}G_{F,G} = \frac{1}{\tau_{FG}S + 1} \quad (1)$$

The time constant used to model this mechanism in such works was  $\tau_{F,G} = 0.5$  s.

In order to more accurately identify and model the different mechanisms taking place within the GENESIS core, a dedicated investigation is conducted. To correctly account for such dynamical mechanisms is important since this model needs to be used in the compensation functions of the VRF system.

Since the void fraction is estimated in the VRF system by measuring the pressure drop over the core it is important to identify the power to core pressure drop transfer mechanism,

$\delta q$ -to- $\delta dP_C$ . A block representation of this process is shown in Fig. 3.

The first two transfer functions, which need to be compensated for, correspond to the dynamics of the GENESIS heating rods  $G_{F,G}$ , and the vapor production process in Freon  $G_{vp,G}$ . The last transfer function named  $G_{tt,G}$ , is related to the transport of the coolant through the core, which is responsible of the measured pressure drop. This last process associated to the mass transport through the core has not to be compensated because it is correctly simulated in GENESIS since the axial dimensions, the void fraction profile and the mass flow rate, are properly considered in the downscaling (Marcel et al., 2007).

The investigation regarding the characterization of the processes shown in Fig. 3 is divided into two parts. First, a numerical estimation of the dynamics of the heating rods and the mass transport in the core is performed. Second, the estimated time constants associated to those processes are used as initial guesses for the fitting of the parameters of the transfer function from  $\delta q$ -to- $\delta dP_C$ , i.e.  $G_{power-dPc} = G_{F,G} G_{vp,G} G_{tt,G}$  presented in Fig. 3.

A numerical 1D model (Degen, 2006) is used to describe the GENESIS rod dynamics (represented by  $G_{F,G}$  in Fig. 2) following the same procedure as in the reactor fuel rods case, see (Marcel et al., 2007). In order to have a good representation of the dynamics of the heating rods in a broad range of frequencies, a second order transfer function was proposed to be implemented. This model is expected to more efficiently capture the fast dynamics taking place in the rods which might be of importance in stability, as suggested in Van der Hagen (1988). Therefore,

$$G_{F,G} = \frac{A_1}{(1 + \tau_{F,G,1}S)(1 + \tau_{F,G,2}S)} \quad (2)$$

After fitting the response of the heat flux at the rod surface, after a power step is applied to the rod, the following two time constants are found,

$$\begin{aligned} \tau_{F,G,1} &= 0.03s \\ \tau_{F,G,2} &= 0.28s. \end{aligned} \quad (3)$$

The boiling process is assumed as a first order process. This is supported by the fact that boiling heat transfer mechanism in Freon is less efficient than that in water (Van Stralen and Cole, 1979) and therefore affects the dynamics of the process, which can be considered as instantaneous in water but not in Freon. The first order model assumption together with the second-order representation of the fuel rods has demonstrated to provide a very good representation of the process to be compensated for, as it will be shown later. Thus,

$$G_{vp,G} = \frac{A_2}{(1 + \tau_{vp,G}S)} \quad (4)$$

The transfer function representing the coolant flow through the core  $G_{tt,G}$  can be approximated with a first order model with an associated time constant  $\tau_{tt,G}$  equal to the effective transit time of the flow through the core (Earni et al., 2003).

$$G_{tt,G} = \frac{A_3}{(1 + \tau_{tt,G}S)} \quad (5)$$

This transit time is calculated as in Marcel et al., 2007 by using the next set of conditions.



Fig. 3. Schematic representation of the power to core pressure drop transfer mechanism.

$$\begin{aligned} N_{\text{PCH}} &= 5.7 \\ N_{\text{Sub}} &= 1.2 \\ M &= 0.62 \text{ kg/s} \end{aligned} \quad (6)$$

The corresponding effective fluid transit time in the core is found to be

$$\tau_{\text{tt,G}} = 0.45 \text{ s} \quad (7)$$

The transfer function for the mechanism described in Fig. 3 is thus,

$$G_{\text{power-dPc}} = \frac{A}{(1 + s0.03 \text{ s}^{-1})(1 + s0.28 \text{ s}^{-1})(s\tau_{\text{vp,G}} + 1)(1 + s0.45 \text{ s}^{-1})} \quad (8)$$

where  $A = A_1 A_2 A_3$ .

For the second part of this study, two signals are used (which are obtained at the conditions detailed in Eq. (6) and the VRF system turned off): the electrical power input, to which a white noise with amplitude of 6% is added  $\delta q$ , and the signal from the fast response dP sensor located across the core  $\delta \text{dP}_c$ . The cross correlation between these two measured signals  $\text{CCF}_{\text{meas}}$  is calculated and presented in Fig. 4.

The peak located at  $\sim 0.67 \text{ s}$  is found to be associated to the phenomena indicated in Fig. 3.

In addition, a relation exists between measured vapor and flow fluctuations. Since the flow is merely driven by natural circulation, an increase in the vapor production influences the flow by increasing buoyancy in the system. The second peak located at  $\sim 4 \text{ s}$  seems to reflect this feedback mechanism. This reasoning can be confirmed since the distance between the two positive peaks ( $\sim 3.3 \text{ s}$ ) agrees well with the traveling time found for the chimney section (3.24 s). Since the feedback due to buoyancy can be well discriminated from the fast processes occurring in the core, it is ignored in the following analysis.

The estimated transfer function  $G_{\text{power-dPc}}$  is used with the noisy power to-heat flux  $\delta q$  as input to obtain an estimated pressure drop over the core  $\delta \text{dP}_{c,\text{est}}$ . The Simulink tool from the MATLAB environment is used for that purpose. A second cross correlation  $\text{CCF}_{\text{est}}$  is calculated with these two signals and compared with the previous  $\text{CCF}_{\text{meas}}$ . All the time constants present in  $G_{\text{power-dPc}}$  (see Eqs. (2), (4) and (5)) are varied until the similarity between  $\text{CCF}_{\text{meas}}$  and  $\text{CCF}_{\text{est}}$  is optimized, i.e. the error of  $\text{CCF}_{\text{est}}$  for the first peak is minimal. The resulting  $\text{CCF}_{\text{meas}}$  is also plotted in Fig. 4.

Table 2 summarizes the time constants estimated analytically and their correspondence with the ones found through the fitting

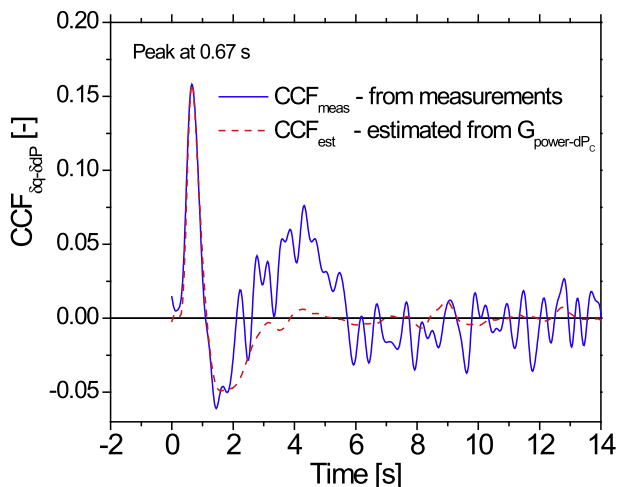


Fig. 4. Cross correlation function of the noisy power input and the dP measured across the core (solid line) and the analytical estimation (dotted line).

process. By comparing the experimental and analytical time constants it can be seen that a very good agreement exists for the first peak. It can therefore be concluded that the modeled physical mechanisms present in the heated section are well characterized.

Since the processes occurring in the GENESIS core are successfully modeled, the compensation transfer function presented in Eq. (9) (based on the experimental analysis presented above) can be expressed in the  $z$  domain (the discrete version of the Laplace variable  $s$ ) and implemented in the VRF system algorithm.

$$\begin{aligned} G_{F,G}^{-1}(s)G_{\text{vp,G}}^{-1}(s) &= G_{\text{power-dPc,G}}^{-1}(s)G_{\text{tt,G}}(s) \\ &= \frac{(1 + s3.2\text{s}^{-1})(1 + s3.57\text{s}^{-1})(1 + s49.9\text{s}^{-1})}{sA'} \end{aligned} \quad (9)$$

with  $A' = 3.37 \times 10^{-3} \text{ 1/W}$ .

The following results are obtained by using the improved compensation transfer function expressed in Eq. (9).

### 3. Parametric study

In this section, the capabilities of the GENESIS facility are exploited by modeling different fuel rods, varying the void reactivity coefficient and changing some operational parameters, such as the pressure and the feedwater sparger location. Unless indicated, the power and inlet subcooling (defining the operational point in the dimensionless plane) are the same for all experimental cases and correspond to a reference situation of the GENESIS facility, named as REFERENCE CASE, which is characterized by:

$$\begin{aligned} N_{\text{PCH}} &= 5.7 \\ N_{\text{Sub}} &= 1.2. \end{aligned} \quad (10)$$

All the stability results presented in this work are obtained by using noise analysis. Details of the treatment of the data and the procedure followed in the analysis can be found in Marcel et al., 2007.

#### 3.1. Effect of the improved VRF system

This study is intended to investigate the influence of using the compensation function expressed in Eq. (9) instead of the simple one expressed by Eq. (11) used in previous works (Rohde et al., 2010, 2007; Furuya et al., 1635; Marcel et al., 2008) which assumes a first order model of the phenomena involved.

$$G_{\text{vp,G}}^{-1}G_{F,G}^{-1} = \frac{\tau_{F,G}s + 1}{1} \quad \text{with } \tau_{F,G} = 0.5 \text{ s} \quad (11)$$

The stability obtained by using the VRF system with both algorithms is presented in Table 3.

As can be seen, implementing the simple compensation function from Eq. (11) seems to have a non-conservative effect since the decay ratio (DR) is underpredicted compared to the one obtained from the new implementation which assumes a third-order model for the process to be compensated for ( $G_{F,G} G_{\text{vp,G}}$ ). Interestingly the resonance frequency remains unchanged. As it will be shown later, a slower dynamics of the heat transfer from the rods to the coolant increases the neutronic-thermal-hydraulic stability.

The result found in this section indicates that care has to be taken when compensating a higher order system by a lower order transfer function since this election may lead to non-conservative results.

#### 3.2. Effect of the modeling of the reactor fuel rods

Van der Hagen has proposed that the dynamics of heat transfer taking place in a BWR core during Type-II oscillations is governed

**Table 2**  
Experimentally and analytically found parameters of the TF from Fig. 2.

Physical process	Parameter	Numerical value	Experimentally derived value	Previous implementation
Heat transport within the rod	$\tau_{FG,1}$	0.03 s	0.02 s	0.5 s
	$\tau_{FG,2}$	0.28 s	0.28 s	
Boiling process	$\tau_{vpg}$	Unknown	0.31 s	
Void transport through the core	$\tau_{ttG}$	0.45 s	0.45 s	–

**Table 3**  
Experimental decay ratio and resonance frequency found for the reference case by using the VRF system with the compensation functions described in Eq. (11) and the more sophisticated ones developed in this work and expressed in Eq. (9).

$r_\alpha = -0.103$	DR [-]	$f_{res}$ [Hz]
REFERENCE CASE – VRF using Eq. (9)	$0.31 \pm 0.02$	$0.66 \pm 0.02$
VRF using Eq. (11)	$0.26 \pm 0.02$	$0.66 \pm 0.03$

by small fuel time constants that are associated with heat transfer from the outer region of the fuel rods (Earni et al., 2003). It is therefore important to investigate the stability effect when modeling the heat transfer within the fuel rods by using a first order model since in this case the rod dynamics is described by only one time constant. The GENESIS facility is therefore used with a first order implementation of the ESBWR rods. The associated time constant is obtained by fitting with a first-order-model the analytic solution of the transient temperature response due to a step in the applied power, as detailed in Marcel et al., 2007. Experiments obtained at the same operational conditions as the reference case are conducted by using this new rods implementation. As a matter of completeness, such rods are also implemented and tested in the VRF using compensation functions described by Eq. (11). The results of this study are shown in Table 4.

It is observed that by using a first order transfer function to model the reactor fuel rods stabilize the system for both cases, when using the new third-order implementation developed in this work and also with the VRF model using Eq. (11). This effect is due to the fact that by using a slow representation for the fuel rods filters out the dynamics of the power-to-vapor production effect which is important in the neutronic-thermal-hydraulic instability mechanism.

From the experiments it can be concluded that by representing the fuel rods using a first order model approximation with the fitted time constant leads to non-conservative results. It therefore can be confirmed that the effective time constant that has to be used if a first order model is selected for the rod modeling, is associated to fast responses taking place in the fuel rods (defining the effective time constant as the time constant corresponding to a first order model which would give the same stability results as the real system).

Another option would be to represent the fuel rod dynamics as (at least) a second-order system in order to avoid undesired effects originated from the modeling of such a component.

Table 4 also shows that the use of the VRF implementation which uses Eq. (11) as compensation functions reinforces the stabilization effect caused by approximating the fuel rods as first order systems, as discussed in Section 3.1.

**Table 4**  
Experimental decay ratio and resonance frequency found for the reference case (which uses a 2<sup>nd</sup> order representation of the fuel rods) and the case in which a 1<sup>st</sup> order model for describing the ESBWR fuel rods is used.

$r_\alpha = -0.103$	$\tau_{F,1}$ [s]	$\tau_{F,2}$ [s]	DR [-]	$f_{res}$ [Hz]
2 <sup>nd</sup> order approx. REFERENCE CASE	0.57	6.55	$0.31 \pm 0.02$	$0.66 \pm 0.02$
1 <sup>st</sup> order approx.	4.86	$0.24 \pm 0.03$	$0.64 \pm 0.02$	
1 <sup>st</sup> order approx. + VRF with Eq. (11)	4.86	$0.20 \pm 0.02$	$0.64 \pm 0.02$	

From now on the so-called REFERENCE CASE refers to the experiment results obtained with the new VRF system which uses the compensation functions described by Eq. (9) and also the second order model of the reactor fuel rods.

### 3.3. Effect of changing the rod diameter

The impact of changing the fuel rod diameter on the stability performance is investigated in this section. For this purpose two cases are studied and afterward compared with the reference case: a case in which the fuel rods diameter is twice the one from the reference case and a case in which the diameter is half of that. Different authors have predicted that when modeling the fuel rods as first order systems, large time constants (*large* compared to typical periods of thermal-hydraulic instabilities) have a stabilizing effect on Type-II oscillations because of a significant filtering of high-frequency oscillations in the void reactivity feedback loop (Bragt et al., 1998b; Furuya et al., 2004). However, to what extent this holds for a second-order approximation of the fuel rod dynamics, is not known. The results of this study are condensed in Table 5.

Having the doubled diameter fuel rods stabilizes the system while decreases the resonance frequency. This effect can be understood by the lower cut off frequencies associated to thicker rods, which filters more effectively the high frequency fluctuations induced by the void reactivity feedback dynamics. For the same reason, the typical frequency associated to this type of rod is lower. The opposite occurs in the experiments when modeling the fuel rods having a diameter being half the reference one. However, these differences are found to be less pronounced than those predicted by numerical models using a first order approximation for the rods dynamics (Degen, 2006). This effect seems to be related to the larger time constant derived from the first order approximation which tends to amplify the differences in the dynamics of the rods. As a result of this, it is likely possible that numerical investigations using a first order approximation for the fuel rods (see for instance Bragt et al., 1998b) may overpredict the effect of rod diameter on stability.

### 3.4. Effect of using a MOX fuel

The recycling of plutonium as mixed oxide (MOX) has a promising potential for reducing the long-term radiotoxicity of disposed nuclear fuel. For this reason, the use of MOX fuel in light water reactors is an important part of the nuclear strategy in many countries worldwide. It is thus of importance to investigate the influence on the stability performance when MOX fuels are loaded in a BWR. In this section, the stability behavior of the reference reactor being fully loaded with a typical MOX fuel is investigated by

**Table 5**

Experimental decay ratio and resonance frequency found for the reference case and two cases using different fuel rod diameters.

$\Gamma_{\alpha} = -0.103$	$\tau_{F,1}$ [s] <sup>†</sup>	$\tau_{F,2}$ [s] <sup>†</sup>	$\tau_F$ [s] <sup>‡</sup>	DR [-]	$f_{res}$ [Hz]
$D_{rod} = 2.0 D_{rod REF}$	1.31	17.65	14.05	$0.28 \pm 0.02$	$0.62 \pm 0.02$
REFERENCE CASE	0.57	6.55	4.86	$0.31 \pm 0.02$	$0.66 \pm 0.02$
$D_{rod} = 0.5 D_{rod REF}$	0.22	2.04	1.67	$0.34 \pm 0.01$	$0.67 \pm 0.03$

<sup>†</sup> Obtained by fitting the analytical solution with the solution for a second order system.<sup>‡</sup> Idem before but with the solution for a first order system (not used in the experiments).

slightly changing the VRF system implementation in the GENESIS facility. MOX fuel at the beginning of the cycle (BOC) is considered which is known to have the most different neutronic behavior regarding UO<sub>2</sub> fuel (Demazière, 2002). Since the geometrical and thermo-physical properties (relevant for the heat transfer mechanisms) of the MOX fuels are practically the same as those for a fuel filled with UO<sub>2</sub> pellets at BOC and MOC respectively (Bailly et al., 1999) the implementation of the fuel rods remain unchanged. In order to account for the different neutronic behavior of the MOX fuel, the neutronic parameters needed for the six groups point kinetics model implemented in the algorithm are obtained from numerical simulations when using a reference neutron flux (Leppanen, 2005). The MOX fuel composition and the resulting neutronic parameters are given in Tables I and II from the Appendix.

From SIMULATE-3 calculations, Demazière estimated the moderator temperature coefficient (for which the void reactivity coefficient is the largest contributor) to be 15% larger for a fully loaded MOX fuel core at BOC than the correspondent UO<sub>2</sub> one at MOC (Demazière, 2002; Kloosterman and Kuijper, 2000). In this investigation, the void reactivity feedback coefficient for the MOX experiment is therefore 1.15 times the void reactivity coefficient used for the reference case.

The results of the stability performance of a core fully loaded with MOX and the reference case in which UO<sub>2</sub> fuel is used are presented in Table 6.

It can be seen that the MOX fuel causes the system to be slightly more unstable and shows a higher resonance frequency than that using a conventional UO<sub>2</sub> fuel. This difference can be attributed to the smaller effective delayed neutron fractions from MOX fuels, mainly caused by the <sup>239</sup>Pu and <sup>240</sup>Pu content and the larger moderator temperature coefficient.

### 3.5. Effect of the pressure

In (Marcel et al., 2007) it has been shown that the scaling factors used in the design of the GENESIS facility are hardly dependent on the system pressure for pressures close to the design value (11.4 bar). Based on this, GENESIS can be used to explore the thermal-hydraulic stability performance of a natural circulation loop when the operational pressure shifts to higher or lower values. By changing the pressure, the fluid properties change, particularly the vapor density and the saturation temperature. The inlet subcooling and the power input were therefore adjusted in such a way the operational point in the non-dimensional plane was kept the same. If those parameters were not kept constant, the GENESIS working point would be different and therefore no comparison could be made between the cases. The results of the

**Table 6**

Experimental decay ratio and resonance frequency found for the reference case and the case simulating a core fully loaded with MOX fuel.

	DR [-]	$f_{res}$ [Hz]
REFERENCE CASE (UO <sub>2</sub> fuel, $\Gamma_{\alpha} = -0.103$ , $\beta = 0.00562$ )	$0.31 \pm 0.02$	$0.66 \pm 0.02$
MOX case (MOX fuel, $\Gamma_{\alpha} = -0.118$ , $\beta = 0.004079$ )	$0.33 \pm 0.05$	$0.91 \pm 0.02$

investigation regarding the pressure effect on the system stability (obtained without reactivity feedback) are shown in Table 7.

From the table, no clear change is observed in the resulting stability. This finding agrees well with numerical calculations obtained by Van Bragt who found very little dependency of the stability boundary when varying the system pressure in the modeled natural circulation channel (Van Bragt et al., 1998). Such a finding valid for natural circulation systems is due to the fact that there is no explicit pressure dependency on the dimensionless parameters which determine the stability of the system (see Marcel et al., 2007). Since all the dimensionless numbers are kept the same (the inlet coolant temperature and the power are adjusted to have the same  $N_{PCH}$  and  $N_{Sub}$ ) the stability boundary location is also preserved. In addition to this issue, it is worth mentioning that the main source of uncertainties in the experiments was related to perturbations in the system pressure introduced by the pressure controller. Great effort was put into reducing this problem. An excellent solution was obtained by adding a second controlling system with a much smaller control valve put in parallel with the existing one and adjusting the feedback gains of the closed loops.

### 3.6. Effect of the feedwater sparger position

Zboray and Podowski have shown that fluctuations in the core inlet coolant temperature can significantly influence the stability of closed-loop reactor systems (Zboray et al., 2001; Podowski and Pinheiro Rosa, 1997). As a result of numerical investigations, Zboray has found that natural circulation boiling systems change their stability performance when the feedwater sparger position is varied (Zboray et al., 2001). In the case in which the sparger position is placed at the core inlet, he predicted the system to be unconditionally stable regarding the thermal-hydraulic stability mode. Zboray found that in his model the influence of flow variations on the boiling-boundary position is cancelled out by the influence of the core inlet-temperature variations if the sparger position approaches to the core inlet. In order to investigate such a prediction, the GENESIS facility is destabilized by increasing the chimney outlet local restriction which would amplify any instability mechanism induced by density waves travelling through the chimney. The thermal-hydraulic stability performance of this new configuration (the so-called DESTABILIZED CASE) is investigated for three feedwater sparger inlet positions, which are located at different heights regarding the core inlet (see Fig. 1). The stability results for these experiments (obtained without reactivity feedback) are presented in Table 8.

From the experiments it is seen that when lowering the feedwater sparger position, the stability performance is affected. By inves-

**Table 7**

Experimental decay ratio and resonance frequency found when varying the pressure while keeping the same operational point in the dimensionless plane.

$\Gamma_{\alpha} = 0$	DR [-]	$f_{res}$ [Hz]
Low Pressure (6.6 MPa-water equivalent)	$0.02 \pm 0.05$	$0.15 \pm 0.03$
REFERENCE CASE (7.1 MPa-water equivalent)	$0.09 \pm 0.04$	$0.13 \pm 0.03$
High Pressure (7.4 MPa-water equivalent)	$0.07 \pm 0.03$	$0.16 \pm 0.04$



**Table 8**

Decay ratio and resonance frequency found for the destabilized case using three different feedwater sparger positions.

DESTABILIZED CASE – $r_{\alpha} = 0$	DR [-]	$f_{res}$ [Hz]	$\phi$ [°]
<sup>†</sup> FW sparger at 7.3 m (Nominal position)	$0.60 \pm 0.02$	$0.108 \pm 0.002$	-253
<sup>†</sup> FW sparger at 3.3 m	$0.83 \pm 0.02$	$0.106 \pm 0.002$	-168
<sup>†</sup> FW sparger at 0.3 m	$0.75 \pm 0.02$	$0.110 \pm 0.003$	-110

<sup>†</sup> With respect to the core inlet (See Fig. 1)

tigating the correlation between the signal from the coolant inlet temperature and the signals corresponding to the primary flow, and the feedwater flow and temperature, it is concluded that the core inlet temperature fluctuations, and thus the boiling boundary location, are induced by changes in the primary flow and not by the feedwater flow dynamics.

Zboray related the system stability to the phase between the core inlet temperature and flow fluctuations  $\phi$ , which can be estimated by Podowski and Pinheiro Rosa (1997),

$$\phi = -2\pi f_{res} t_t \tag{12}$$

where  $t_t = \rho_{liq} A_{DC} l_{Sparger} / M_{C,in}$  is the coolant transit time from the sparger position to the core inlet,  $A_{DC}$  is the downcomer cross sectional area and  $l_{Sparger}$  is the distance between the feedwater sparger and the core inlet. Note that  $l_{Sparger}$  is different from the height at which the sparger inlet is located because of the extra piping connecting the downcomer with the core inlet. The resulting phases for the three cases are shown in the last column of Table 8.

Clearly the most unstable case is the one having a phase close to  $-180^\circ$ . For such a value, the inlet-temperature oscillations are out-of-phase with the flow oscillations and therefore reinforce their influence on the boiling boundary oscillations, which are known to have a destabilizing effect on the system. This result seems to confirm the instability mechanism predicted by Zboray.

The stability effect of varying the sparger inlet position can be used to optimize the stability regarding the thermal-hydraulic instability mode. It has to be mentioned, however, that placing the sparger inlet at a too low position may have negative effects on the reactor safety, since in such a case the risk of a loss of inventory accident due to siphon drainage problems is increased.

**3.7. Effect of the void reactivity feedback coefficient**

The influence of the void reactivity feedback coefficient  $r_{\alpha}$  on the stability of the coupled neutronic-thermal-hydraulic reactor

system has been investigated by using both numerical and experimental tools by Zboray and Furuya. Those early works are extended here for the case of a novel natural circulation BWR prototype. Two configurations are studied: The reference case used in Sections 3.1–3.5 and the destabilized case from Section 3.6.

For simplicity, in the following discussion the value of  $r_{\alpha}$  is considered in an absolute sense, thus, omitting its negative sign.

The experiments are obtained by operating the GENESIS facility in the two aforementioned configurations and varying  $r_{\alpha}$  step by step, ranging from 0 (no neutronic feedback effect) to twice the nominal value. The resulting trends in the DR and in the  $f_{res}$  are depicted in Fig. 5.

In the reference case a clear increase in the  $f_{res}$  can be observed when increasing  $r_{\alpha}$ . The value of  $f_{res}$  is then stabilized for  $r_{\alpha}$  above the nominal value of  $r_{\alpha} = -0.103$ . In this case the larger  $r_{\alpha}$  the more unstable the system is. This effect is explained as follows. At  $r_{\alpha} = 0$  the only instability mechanism present in the system is attributed to density waves traveling through the core plus chimney sections, with an associated low  $f_{res}$ . When the neutronic feedback mechanism is included, another instability mechanism appears which is related to the vapor transport through the core section only. This process is faster than the previous one which explains the higher frequency at larger values of  $r_{\alpha}$ . The relative stabilization of the  $f_{res}$  value is explained by fact that the vapor transport in the core remains unchanged since the working point of the facility is the same for all cases. The trend of the DR is due to the fact the thermal-hydraulic mode is extremely stable for this configuration (see the low DR value corresponding to  $r_{\alpha} = 0$ ) when compared to the reactor-kinetic instability mode. By increasing the value of  $r_{\alpha}$  the reactor-kinetic instability mode becomes more important and thus the DR increases. Interestingly the shift from one instability mechanism to the other one is smooth as it is revealed by the  $f_{res}$  and the DR trends.

For the thermal-hydraulic destabilized case it can be seen that, as a result of the variations in the void reactivity coefficient, the system exhibits a complex behavior. In this case, the system is less stable than in the reference case regarding the thermal-hydraulic mode since the DR is larger when  $r_{\alpha} = 0$ . Increasing  $r_{\alpha}$  clearly affects the stability performance. In particular, a transition region characterized by fluctuations in the obtained value of the DR is found for  $-0.06 < r_{\alpha} < -0.03$ . A strong effect can be observed on  $f_{res}$  in this region, even for very small values of  $r_{\alpha}$ . When increasing the importance of the neutronic feedback mechanism (i.e. increasing  $r_{\alpha}$ ) in the range of  $-0.15 < r_{\alpha} < -0.06$  the system shows a slight increase in the stability performance while the value of  $f_{res}$  corresponds to the Type-II neutronic-thermal-hydraulic mode.

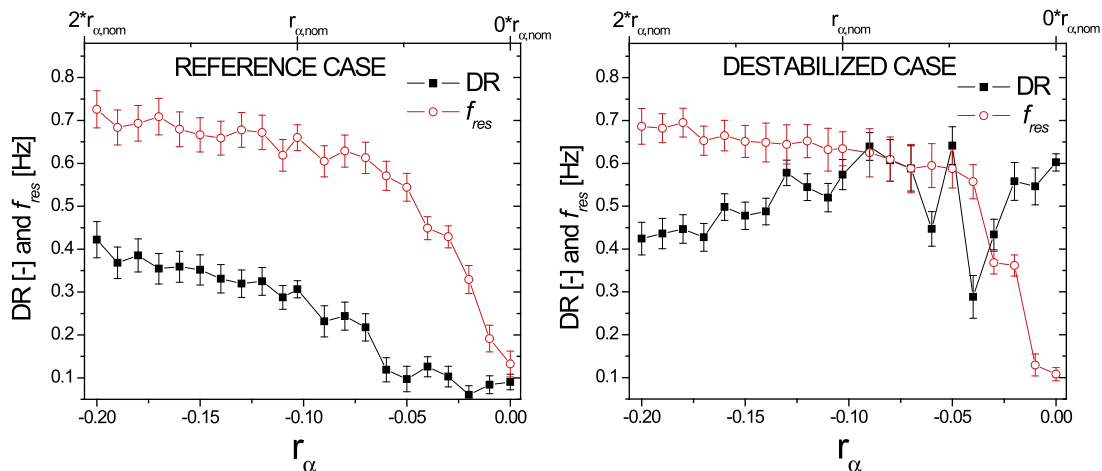


**Fig. 5.** Effect of varying the void reactivity coefficient in the system stability.

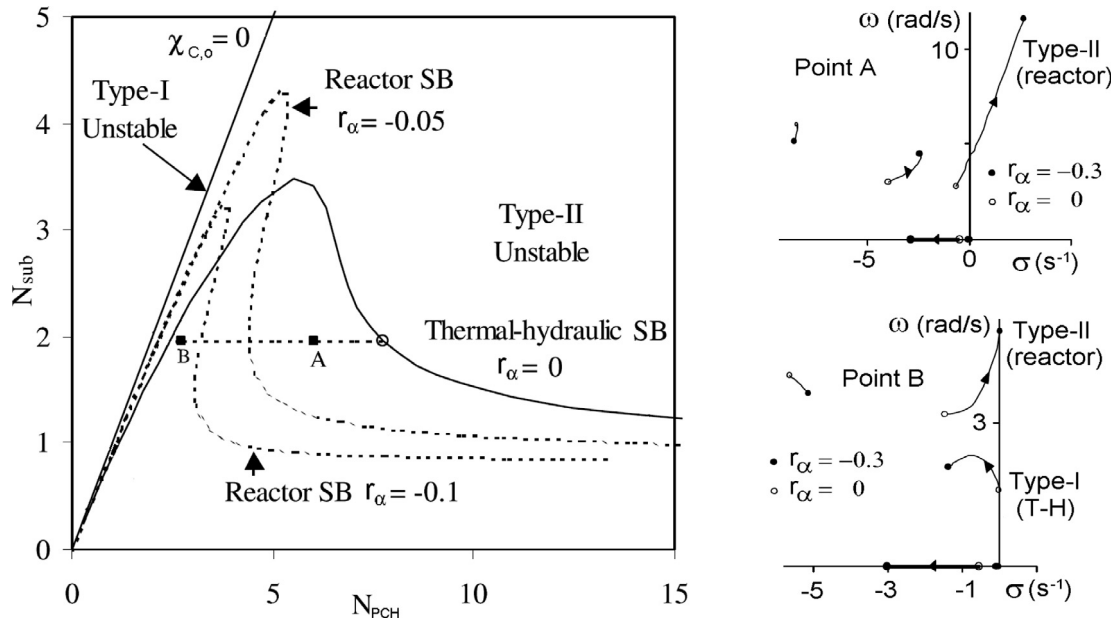


Fig. 6. Stability map for different values of the void reactivity coefficient obtained by Zboray (Van Bragt et al., 1998). The root-loci corresponding to the points A and B are also presented.

In order to understand these findings, numerical results obtained by Zboray with a reduced order model are recalled (Zboray, 2002). Fig. 6 shows the stability maps obtained when different void reactivity coefficients are used in the numerical simulations. The root-loci diagrams corresponding to the points A and B are also included in the left hand side plots.

The reference case can be related to the point A in the stability map since it corresponds to a relatively stable system from the thermal-hydraulic point of view. From the root-loci diagram, it is seen that for  $r_\alpha = 0$  the thermal-hydraulic stability mode dominates but as soon as  $r_\alpha < 0$ , the pole associated to the reactor instability mode moves to the right, destabilizing the system.

The behavior of the so-called destabilized case can be compared to the point B in the stability map since it describes a relatively unstable system regarding the thermal-hydraulic instability mode. In this case, the root-loci shows that for  $r_\alpha = 0$ , the pole associated to the reactor-kinetic mode is rather far from the unstable half plane. In contrast, the pole related to the thermal-hydraulic mode is close to the stability boundary and therefore dominates. By increasing the value of  $r_\alpha$  the reactor-kinetic pole moves to the right and the thermal-hydraulic pole moves to the left. As a result of this, a range of  $r_\alpha$  values with associated low DR values is found. This phenomenon can therefore be associated to the interchange of the importance of the poles corresponding to the two instability modes. Consequently, a range of  $r_\alpha$ 's with low DRs is found.

In the GENESIS experiments two different resonance frequencies exist which can be related to the fluid transit time through the core plus chimney sections and the core section only, corresponding to the thermal-hydraulic oscillatory mode ( $f_{res,T-H} \approx 0.15$  Hz) and the reactor oscillatory mode ( $f_{res,R} \approx 0.75$  Hz) respectively. In order to further investigate the trend from one mode to the other one, the normalized power spectral decomposition of the detrended flow inlet signal obtained for the reference case, is analyzed and shown in Fig. 7.

As indicated before, the resulting frequency  $f_{res}$  varies from the low frequency value, corresponding to the thermal-hydraulic mode (T-H mode), to higher frequencies in which the reactor oscillatory mode is dominant. In order to point this

out, the trend of the resonance frequency is also superimposed in the figure. As soon as  $r_\alpha < 0$ , the effects of the T-H mode are strongly diminished since the PSD function at such low frequencies is drastically reduced (i.e. the PSD broadens, diminishing the power at the resonance frequency of the T-H mode). This result agrees with the strong stabilization of the T-H mode observed in the destabilized case when the VRF system is included. In contrast to this, when  $r_\alpha$  approaches its nominal value ( $r_{\alpha, nominal} = -0.103$ ) the neutronic feedback is of importance, causing the reactor mode to be dominant.

In order to better characterize the experiments, the results are divided into three groups according to the shape of the PSD functions. The resulting PSD's are shown in Fig. 8.

It is observed that the first low frequency region, which is associated with the T-H mode, is characterized by only two cases corresponding to zero or very low values of  $r_\alpha$ . The region located at

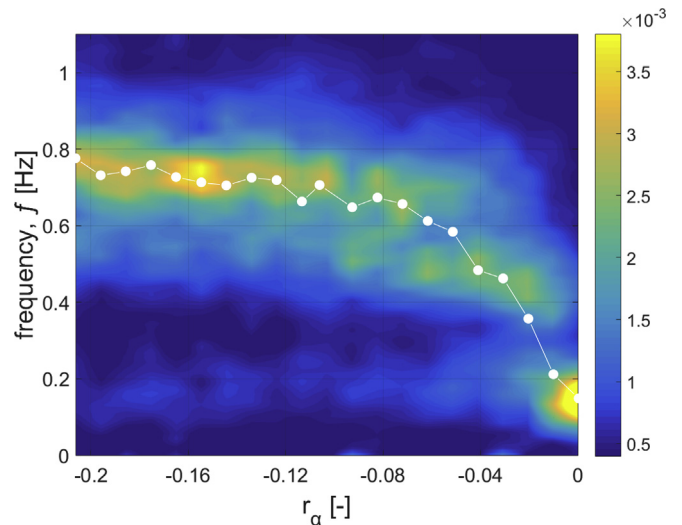


Fig. 7. PSD of the inlet flow signal for different values of  $r_\alpha$ . The corresponding resonance frequency is also superimposed in the plot.

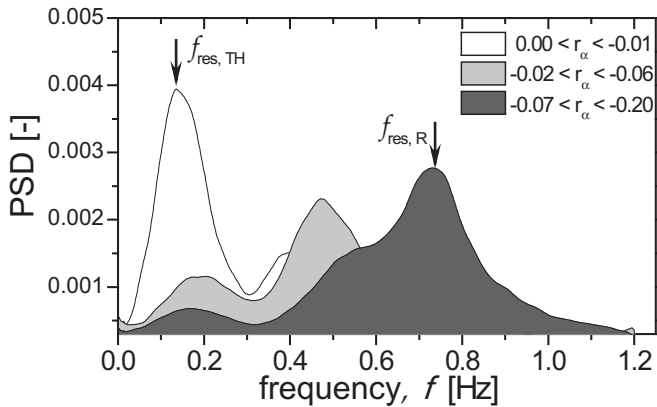


Fig. 8. PSD plots obtained when grouping the results according to three different regions of  $r_\alpha$ . The resonance frequency of the two identified oscillatory modes is also shown in the plot.

intermediate frequencies is defined by the cases with  $r_\alpha$  between  $-0.02$  and  $-0.06$ . The existence of this peak has not been reported in the past and may be related to a new feedback mechanism. Further investigations are needed to elucidate this issue. Its location coincides with an intermediate frequency between the T-H mode and the reactor mode ( $f_{res} \approx 0.45$  Hz). The third region groups the experiments obtained with  $r_\alpha$  between  $-0.07$  and  $-0.20$ . This peak is associated with the void-neutronic feedback mechanism and its location can be related to the time for the heat transport within the rods plus the boiling process and the transport of such a vapor through the core section.

#### 4. Conclusions

As a result of the parametric study which uses the advanced implementation of the VRF system developed in this work, the following conclusions could be drawn:

- When using a first order model for deriving the compensation function of the heating rods in the VRF system, care has to be taken on selecting the appropriate time constant since this parameter influences the resulting stability performance.
- Modeling the reactor fuel rods as a first order system (with the time constant obtained by fitting the time response with a first order solution) leads to a too low estimate of the decay ratio (DR). A higher order model implementation is therefore needed to avoid erroneous results.

From the parametric study, it can be concluded that:

- Changing the fuel rods diameter to a half (doubling) decreases (increases) the stability performance of the system while the resonance frequency increases (decreases). This effect is probably be less pronounced than when the fuel rods are modeled as first order systems because in the last case the rods more effectively filters high-frequencies which are of relevance for Type-II instabilities.
- The use of MOX fuels in a BWR seems to slightly decrease the stability performance of the reactor since the smaller effective delayed neutron fraction brings the system closer to prompt-criticality. In addition, the resonance frequency is found to be higher than that for  $\text{UO}_2$  fuels.
- The pressure has little influence on the thermal- hydraulic stability of the system when expressed in the dimensionless plane (for  $66 \text{ bar} < P < 74 \text{ bar}$ ).

- Lowering the position of the feedwater sparger position affects the thermal-hydraulic stability of the system. This effect may be used to optimize the stability margin of the reactor regarding that instability mode.
- Small values of the void reactivity feedback coefficient may strongly affect the thermal-hydraulic instability mechanism.
- A strongly destabilized system regarding the thermal-hydraulic mode can destabilize a reactor when considering the neutronic-thermal-hydraulic mode. The last could be particularly important in accidental situations like in the case of a channel blockage.
- A clear peak is found in the power spectral decomposition of the flow signal at intermediate frequencies (regarding the resonance frequencies of the thermal-hydraulic and the reactor-kinetic instability modes) when the void reactivity coefficient is varied. This may be related to a new feedback mechanism which may be present in natural circulation BWRs. Further investigations are therefore needed in order to confirm the origin of this finding.

#### MOX fuel reference neutronic data

Table I. Composition of the MOX fuel implemented artificially in the GENESIS VRF system (Demazière, 2002).

MOX fuel with 5% Pu loading	
U-234	0.002%
U-235	0.250%
U-238	99.748%
Pu-238	4.000%
Pu-239	50.000%
Pu-240	23.000%
Pu-241	13.000%
Pu-242	10.000%

Table II. Neutronic data corresponding to the point kinetics implementation with six groups of delayed neutrons for the ESBWR UOX fuel (REFERENCE case) provided by GE, and for the EPR (MOX fuel, Leppanen, 2005), obtained by using the VAREX code (Kloosterman and Kuijper, 2000).

	Delay neutrons decay constant ( $s^{-1}$ )	Delayed neutrons fraction [-]	Neutron gen.time ( $\mu s$ )
ESBWRUOX fuel (MOC)	$\lambda_1 = 0.0125$	$\beta_1 = 0.03$	$\lambda = 50$
	$\lambda_2 = 0.0306$	$\beta_2 = 0.21$	
	$\lambda_3 = 0.1150$	$\beta_3 = 0.19$	
	$\lambda_4 = 0.3110$	$\beta_4 = 0.39$	
	$\lambda_5 = 1.2100$	$\beta_5 = 0.13$	
	$\lambda_6 = 3.2000$	$\beta_6 = 0.05$	
$\lambda_{\text{effective}} = 0.09$		$\beta_{\text{Total}} = 0.00562$	
EPRMOX fuel (BOC)	$\lambda_1 = 0.01318$	$\beta_1 = 0.02$	$\lambda = 5.95$
	$\lambda_2 = 0.03054$	$\beta_2 = 0.21$	
	$\lambda_3 = 0.1234$	$\beta_3 = 0.18$	
	$\lambda_4 = 0.3329$	$\beta_4 = 0.37$	
	$\lambda_5 = 1.282$	$\beta_5 = 0.17$	
	$\lambda_6 = 3.479$	$\beta_6 = 0.05$	
$\lambda_{\text{effective}} = 0.08$		$\beta_{\text{Total}} = 0.004079$	

## References

- Bailly, H., Mènesier, D., Prunier, C., 1999. *The Nuclear Fuel of Pressurized Water Reactors and Fast Reactors*. Intercept Ltd.
- Van Bragt, D.D.B., Rizwan-uddin, van der Hagen, T.H.J.J., 1998b. Stability of natural circulation boiling water reactors: Part II-parametric study of coupled neutronic-thermal-hydraulic stability. *Nucl. Technol.* 121.
- Cheung, Y.K., Shiralkar, B.S. and Rao, A.S., "Design Evolution of Natural Circulation in ESBWR", *6th Int. Conference on Nuclear Engineering (ICONE-6)*, San Diego, USA, (1998).
- Degen, C., Dynamics of the GENESIS fuel rods (Bachelor thesis), (2006).
- Demazière, C., Reactor physics calculations on MOX fuel in Boiling water reactors (BWRs). Proc. 7th Information Exchange Meeting on Partitioning and Transmutation (IEMPT7) (2002).
- Earni, S., Wang, S., Mohan, R., Shoham, O., Marrelli, J., 2003. Slug Detection as a Tool for Predictive Control of GLCC<sup>®</sup> Compact Separators. *J. Energy Resour. Technol.* 125, 145–152.
- Furuya, M., 2006. *Experimental and Analytical Modeling of Natural Circulation and Forced Circulation BWRs* (Ph.D thesis). Delft University of Technology.
- Furuya, M., Inada, F., Van Der Hagen, T.H.J.J., 1635. Development of SIRIUS-N facility with simulated void-reactivity feedback to investigate regional and core-wide stability of natural circulation BWRs. *Nucl. Eng. Des.* 235 (15), 1635.
- Furuya, M., Inada, F., Van., der Hagen, T.H.J.J., 2004. Characteristics of type-I density wave oscillations in a natural circulation BWR at relatively high pressure. *J. Nucl. Sci. Technol.* 42 (2), 191–200.
- Ishii, M., Revankai, S.T., Dowlati, R., Bertodano, M.L., Babelli, I., Wang, W., Pokharna, H., Ransom, V.H., Viskanta, R., Wilmarth, T., Han, J.T., Scientific Design of Purdue University Multi-Dimensional Integral Test Assembly (PUMA) for GE SBWR. NUREG:CR-6309, PU-NE 94:1 (1996).
- Kloosterman J.L. and Kuijper, J.C., VAREX, a code for variational analysis of reactivity effects: description and examples. PHYSOR 200, Seoul, South Korea, October 7–10 2000. ANS.
- Kok, H.V., Van der Hagen, T.H.J.J., 1999. Design of a simulated void-reactivity feedback in a boiling water reactor loop. *Nucl. Technol.* 128.
- Leppanen, J., Preliminary calculations on actinide management using advanced PWR MOX technology, Technical report, VTT, (2005).
- Marcel, C.P., 2007. *Experimental and Numerical Investigations on Natural Circulation Boiling Water Reactors* (Ph.D Thesis). Delft University Press.
- Marcel, C.P., Rohde, M., Van Der Hagen, T.H.J.J., 2007. Fluid-to-fluid modeling of natural circulation BWRs for stability analysis. *Int. J. Heat Mass Transfer* 51 (3–4), 566.
- Marcel, C.P., Rohde, M., Van Der Hagen, T.H.J.J., 2008. Experimental Investigations on the ESBWR Stability Performance. *Nucl. Technol.* 232–244, 164.
- Paladino, D., Auban, O., Huggenberger, M., Candreia, P., Strassberger, H.J., Bandurski, T., Description of PANDA Including Test Matrix, PSI Internal Report TM-42-01-14/ALPHA-01-03-0 (2002).
- Podowski, M.Z., Pinheiro Rosa, M., 1997. Modeling and numerical simulation of oscillatory two-phase flows, with application to boiling water reactors. *Nucl. Eng. Des.* 177, 179–188.
- Rohde, M., Marcel, C.P., Van der Hagen, T.H.J.J., De Haas, D.W., Winkelman, A.J.M., Kaaijk, C.N.J., Manera, A., 2006. Stability study on the ESBWR, Proprietary Report to GE Energy, Nuclear.
- Rohde, M. Marcel, C.P. Manera, A. et al. Experimental and Numerical Investigations on the ESBWR stability Performance. NURETH-12, Pittsburg, USA, Sep. 30 Oct. 4 (2007).
- Rohde, M., Marcel, C.P., Manera, A., Van der Hagen, T.H.J.J., Shiralkar, B., 2010. Investigating the ESBWR stability with experimental and numerical tools: A comparative study. *Nucl. Eng. Des.* 240, 375–384.
- Ruspini, L.C., Marcel, C.P., Clausse, A., 2014. Two-phase flow instabilities: A review. *Int. J. Heat Mass Transf.* 71, 521–548.
- Van Bragt, Rizwan-uddin, D.D.B., Van der Hagen, T.H.J.J., 1998. Stability of natural circulation boiling water reactors: Part I-description stability model and theoretical analysis in terms of dimensionless groups. *Nucl. Technol.* 121.
- Van der Hagen, T.H.J.J., 1988. Experimental and theoretical evidence for a short effective fuel time constant in a boiling water reactor. *Nucl. Technol.* 83, 171.
- Van Stralen, S., Cole, R., 1979. *Boiling Phenomena*. McGraw-Hill, New York.
- Zboray, R., 2002. *An experimental and Modeling Study of Natural-Circulation Boiling Water Reactor Dynamics* (Ph.D thesis). Delft University of Technology.
- Zboray, R., Kruijff, W.J.M., de, Van der Hagen, T.H.J.J., Van Dam, H., 2001. Investigating the stability characteristics of natural circulation boiling water reactors using root loci of a reduced-order model. *Nucl. Technol.* 136 (3).